ELECTROSEISMIC AND SEISMOELECTRIC MEASUREMENTS OF ROCK SAMPLES IN A WATER TANK

Zhenya Zhu, Daniel R. Burns, and M. Nafi Toksöz

Earth Resources Laboratory
Department of Earth, Atmospheric, and Planetary Sciences
Massachusetts Institute of Technology
Cambridge, MA 02139

ABSTRACT

An electromagnetic wave or a seismic wave can induce seismic or electric waves due to the electrokinetic conversion based on the electric double layer in a fluid-saturated porous medium. In this paper, we observe the acoustic fields generated around the electrodes excited by an electric pulse in a water tank. The electroseismic or seismoelectric waves are measured in the water tank system to confirm that the recorded seismic or electric signals are induced in porous samples due to the electrokinetic conversions. The electroseismic and seismoelectric frequency-responses in Berea sandstone and Westerly granite samples are measured at frequency range of 15 kHz to 150 kHz. The experimental measurements show that the effects of the electric source, background noises, and electroseismic or seismoelectric conversions are separated very clearly. We calculate the electroseismic and seismoelectric normalized coupling coefficients in the rock samples and compare them with the theoretical calculation. The variation trends of the normalized coupling coefficients are in agreement with the theoretical predictions. The measurement method in this paper could be used to investigate other electroseismic and seismoelectric properties for petroleum exploration applications.

INTRODUCTION

There is an electric double layer on the interface between solid and fluid in a fluid-saturated porous rock (Morgan et al. (1989); Pride (1994); Pride and Haartsen (1996)). When the fluid is an electrolyte, there are also movable free charges. When a seismic wave propagates in a fluid-saturated porous rock, the seismic wave generates relative movement between the fluid and rock matrix. Consequently, the moving charges induce an electric field. The electric field will be an electromagnetic wave when the seismic wave propagates across an interface which is not continuous in acoustical, electrical, or mechanical properties (Mikhailov et al. (2000); Zhu and Toksöz (2003, 2005)). This process is called a seismoelectric conversion. On the other hand, if there is an electric field in the water or in the fluid-saturated porous rock, the moving charges in the fluid cause fluid movement. This relative movement between solid and fluid generates a seismic wave. This process is called an electroseismic conversion. The seismoelectric and

1

electroseismic conversions are related to the fluid conductivity, rock porosity, permeability, pore size, etc. Seismoelectric and electroseismic measurements made on Earth's surface or in a borehole may provide information about the subsurface properties (Mikhailov et al. (1997); Zhu and Toksöz (2005)). Electroseismic laboratory experiments (Zhu et al. (1994, 1999); Reppert and Morgan (2002)) with scaled layered and borehole models showed that electroseismic waves are induced with electrodes buried in a fluid-saturated formation or in a borehole. Deckman et al. (2005) determined the electroseismic coupling coefficients with a simple measurement cell in the laboratory. Field-scale electroseismic measurements (Thompson (2005); Thompson et al. (2005)) detected possible accumulations of natural gas targets. The results demonstrated discrimination of gas sands at a depth of less than 1000 meters.

Reppert and Morgan (2002) studied the theoretical frequency dependency of electroseismic conversion in a porous medium and derived the frequency-dependent electroseismic voltage coupling coefficient:

$$\frac{\Delta P(\omega)}{\Delta V(\omega)} = \frac{2\varepsilon\xi\kappa}{a}\left(\frac{J_1(\kappa a)}{J_o(\kappa a)}\right)\bigg/\left(\frac{2}{\kappa a}\frac{J_1(\kappa a)}{J_o(\kappa a)}-1\right) \tag{1}$$

where

$$\kappa = \sqrt{\frac{-i\rho\omega}{\eta}}$$

where $\Delta P(\omega)$ and $\Delta V(\omega)$ are the seismic pressure and voltage at angular frequency ω, ε is the dielectric constant, ξ is the zeta potential, a is the pore radius, J is the Bessel function, ρ and η are the fluid density and viscosity, respectively.

The theory shows that the frequency-dependent behavior of the electroseismic conversion is a function of the pore size. The electroseismic conversion from electric energy to seismic energy is related to some important properties of the porous medium, including pore size, permeability, and fluid properties. Studies of electroseismic conversion might provide a new method to explore formation properties with new parameters different from traditional seismic surveys or sonic well logging.

In this paper, we first observe the acoustic fields generated around electrodes excited by a high-voltage electric pulse. We then measure the acoustic fields with and without a rock sample in a water tank to confirm that the electroseismic signals are generated in the porous samples. We measure the electroseismic responses in sandstone and granite at the frequencies of 15 kHz-150 kHz and calculate the voltage coupling coefficients. In the same measurement system, we also measure the seismoelectric conversion in the rock samples. The measured electroseismic and seismoelectric normalized coupling coefficients are compared with the theoretical calculations.

ACOUSTIC FIELDS AROUND THE ELECTRODES

To induce an electric field in a fluid-saturated porous medium, the electrodes must be in contact with the fluid. When a high-voltage pulse is connected to the electrodes, acoustic waves are generated around the electrodes due to the electrothermic effects induced by the currents and thermodilation of water molecules. The physical mechanism involved is similar to lightning and

its associated thunder during a storm. Because this effect is induced by the electric current flow in water, the acoustic wave is not related to the shape and material of the electrodes. We observed the acoustic waves generated by the ring electrodes in a metal water tank in our laboratory. The experimental setup is shown in a 3-D diagram (Figure 1a) and in plan view (Figure 1b). The ring electrodes are made from brass wire with a 1.2 cm inside diameter and a 1.5 cm outside diameter. The movement spacing of the hydrophone (B & K8103) is 2.0 cm/trace. The electric source is a 500 V square pulse 6 μs in width.

Figure 2 shows the acoustic waveforms recorded as the hydrophone moves along three different directions with respect to the electrodes (lines A, B, and C in Figure 1b). From the arrival times and the waveform variation in Figure 2, we confirm that there are two different sets of acoustic waves generated by the positive and negative electrodes, respectively. It should be noted that when recording the waveforms, we use a time delay to avoid the electric influence excited by the source pulse. The amplitude of the electric influence is about 200 times higher than the acoustic signals of interest.

Note that the first arrival from the positive electrode (Figure 2a) is stronger than from the negative electrode (Figure 2b). Because the water tank is metallic, it is connected to ground with certain resistance through the step motors or the attached equipment. Therefore, the electric field around the positive electrode should be stronger than that around the negative electrode.

It is important to note that a current induces an acoustic wave in fluid, which is, in general, an electroseismic conversion between electric and acoustic energies. It is a very important phenomenon to be aware of in all electroseismic measurements, since this effect may stronger than the signals of interest that are related to fluid movement in the pore space.

In a layered model, we observe the electroseismic signals generated around the electrodes and at the interface due to the electroseismic conversion. Figure 3a shows a layered model with epoxy-glued sand and a Lucite block. Five sets of wire electrodes are buried in the sand at different depths. Each electrode set has two electrodes at the same depth with 2.0 cm spacing. The first set of electrodes is at the interface between the sand and Lucite block. The electrodes are excited with a square pulse of 500 V in amplitude, and a P wave transducer records the electroseismic waves at the bottom surface of the Lucite block. The electrodes and model are immersed in a water tank. Figure 3b shows five acoustic waveforms recorded by the transducer when the electric pulse is connected to the electrodes at different depths. From the arrival times in Figure 3b, we see that there are two kinds of acoustic waves, indicated by two arrows. The first wave arrives at the same time (in the time area of 0.038 ms to 0.05 ms). The second wave has higher amplitude, and it arrives at varying times. The first wave with the same arrival time is an acoustic wave generated at the interface between sand and Lucite due to the electroseismic conversion. Because the electric field propagates at a much faster velocity than an acoustic wave, the propagation time from the electrodes to the interface can be ignored. All of the electroseismic waves are converted at the interface, propagate through the Lucite block at its P wave velocity, and then are recorded by the transducer. Therefore, all of the waves arrive at the same time of 0.038 ms, which is the travel time in the Lucite block. The second arrival in Figure 3b has different arrival times depending on the depth of the electrodes. The closer to the interface the electrodes are, the earlier the acoustic wave arrives. From the arrival times we know that the acoustic waves are generated around the electrodes, propagate through the water-saturated glued sand and the Lucite block, and then arrive at the Lucite block's bottom surface. The experimental results confirm that there are two acoustic

waves due to electroseismic conversion. One is induced around the electrodes and then propagates as a seismic wave in the model. The other one is converted at the interface between the sand and the Lucite block. Because the efficiency of electroseismic conversion at an interface is low, the amplitude of the converted seismic wave is weak.

It is very important to separate the two electroseismic waves in any surface electroseismic measurement. The propagation of the seismic wave generated around the electrodes is the same as the traditional seismic survey.

ELECTROSEISMIC SIGNALS GENERATED IN POROUS ROCKS

We next investigate electroseismic signals in porous rock samples in the water tank. These measurements must be made in a large enough container to separate the electroseismic wave induced in the rock samples from the wave generated around the electrodes and any reflection from the container walls.

We apply a single sine burst with high voltage (150V-180V) as the electric source. The center frequency of the electric source varies from 15 kHz to 150 kHz in order to investigate the frequency-dependence of the electroseismic conversion in a rock. The high voltage source will influence the weak electroseismic signals recorded with a hydrophone. If a continuous sine wave were applied as the electric source, however, the electric influence would be too strong to allow extract on the electroseismic signals of interests.

Figure 4 shows the water-tank measurement system in our laboratory. The electrodes are made of silver mesh 5.5 cm by 5.5 cm with 50 cm spacing and located in the middle of the tank. The positive and negative source electrodes connect to the output of a power amplifier to provide the electric source signal. A hydrophone (B & K 8103) is located behind the negative source electrode to avoid the electric influence of the positive source electrode on the hydrophone. Rock samples 2.5 cm thick are placed near the positive source electrode. Two separate point measurement electrodes (V+ and V-) are placed on the two sides of the sample to record the voltage across the sample. The tap-water conductivity is around 0.3-0.8 mS/cm. The distance (not shown in Figure 4) from the hydrophone to the side of the water tank is about 29 cm.

Figure 5 shows the acoustic fields in the measurement system at different center frequencies without any rock sample. First, we record the strong source influence, whose center frequency varies with the source frequency and whose amplitude is much greater than the other signals. From the arrival times, we can determine that the other acoustic arrivals originate from the positive or negative source electrodes as well as the reflections from the back or side walls (shown in Figure 4).

We place the different samples at the position shown in Figure 4 and record the acoustic fields generated by an electric pulse with 100 kHz center frequency and 150 V in amplitude. Figure 6 shows the acoustic waveforms with Lucite, Aluminum, Berea sandstone, limestone, and Coconino sandstone samples, as well as with no sample at all. The parameters of these materials are listed in Table 1. The record with no sample present is also shown, and the acoustic waves generated by the positive and negative electrodes can be seen (trace 1). From the other traces, we can see that the waves generated around the positive electrode arrive earlier than in trace 1 because the P-wave

velocities of the samples are higher than the water velocity. Their amplitudes depend on the transmission coefficients between the sample and water. Around 0.16 ms (Figure 6), we observe the electroseismic signals in traces 4, 5, and 6, induced in the porous rock samples due to the electroseismic conversion in the porous rocks. No signals around 0.16 ms are recorded in traces 3 and 4 because Lucite and aluminum are non-porous and impermeable materials.

Table 1: The parameters of rock samples

Sample name	Density (g/m^3)	P-velocity (m/s)	S-velocity (m/s)	Porosity (%)
Berea sandstone	2.098	2590	1770	19.9
Coconino sandstone	1.819	2790	1800	27.7
Limestone	2.355	3480	2460	9.6
Westerly granite	2.606	4150	2570	0.8

In order to confirm that the acoustic wave recorded at 0.16 ms is the electroseismic signal induced in the rock samples by electroseismic conversion, we place the Berea sandstone sample between the source electrodes and move the sample towards the positive electrode (Figure 7a). Figure 7b shows the acoustic waveforms when the sample moves incrementally. We can calculate the arrival time of the electroseismic signal from the geometry of the measurement system. The amplitudes and arrival times of the electroseismic signal vary only with the sample locations. The closer the spacing between the sample and the positive source electrode, the higher the amplitude. The apparent velocity calculated from the slope on the waveform arrivals is the water velocity of 1480 m/s. The electrode noise and tank reflections do not change during the sample movement.

These experiments confirm that electroseismic signals can be induced in our measurement system and separated from the acoustic waves around the electrode and the influences of the electric source. We may apply our experimental system to measure the electroseismic conversions with the different rock samples and calculate the electroseismic voltage coupling coefficients. The frequency dependence of the voltage coupling coefficients might be applied to study the pore size of the rock samples.

ELECTROSEISMIC VOLTAGE COUPLING COEFFICIENTS

We conduct the electroseismic measurements in the water tank system (Figure 4) with Berea sandstone and Westerly granite samples. Figure 8 shows the electroseismic waveforms recorded with sandstone (Figure 8a) and granite (Figure 8b) under the same normalized scale. In these records, the influences of the electric source are included to show the source frequencies and the high amplitudes compared with the electroseismic signals.

In Figure 8a, the acoustic waves recorded between 0.3 ms to 0.4 ms are induced in Berea sandstone due to the electroseismic conversion. In Figure 8b, the conversion produces weak signals at higher frequencies due to the porosity and permeability of Westerly granite being much lower than sandstone.

Figure 9 records the source electric signals across the samples of Berea sandstone (Figure 9a) and Westerly granite (Figure 9b). The amplitudes of the electric field across the samples are different, but the relative phases are identical. This means the electric characteristics of the rock sample are

equivalent to a pure resistance. The phase shift of the electric waves at different frequencies is due to the phase characteristics of the power amplifier, which provides the high voltage source. When we measure the electroseismic signals in Figure 8, the signals pass through a 60-db-preamplifier. We can determine the frequency response of this preamplifier with a standard function generator and a digital oscilloscope. Then we may correct the amplitudes recoded in Figure 8. The amplitudes ($\Delta P(\omega)$) of the electroseismic signals and the voltage differences ($\Delta V(\omega)$) across the samples can be determined from Figures 8 and 9, then we calculate the electroseismic voltage coupling coefficients ($\Delta P(\omega)/ \Delta V(\omega)$) at the different frequencies.

Figure 10 shows the normalized electroseismic voltage coupling coefficients in Berea sandstone (Figure 10a) and Westerly granite (Figure 10b) at frequencies of 15 kHz to 150 kHz. In the figures we show the theoretical results calculated by Eq. 1, assuming the pore radius of sandstone and granite are 80 μm (Figure 10a) and 20 μm (Figure 10b), respectively. In the theoretical calculation, ρ is $1000\ kg/m^3$, ξ is 80 mV, and η of water viscosity is 8.9×10^{-4} Pa s.

Comparing the experimental result with the theoretical calculation, we see that the variation trends of the electroseismic voltage coupling coefficients are identical. We also see two or three peaks on the experimental coupling coefficients ($\Delta P(\omega)/\Delta V(\omega)$) at different frequencies (Figure 10). The pore size in real rock is not a single value. The two or three peaks in the coupling coefficient are likely due to the different distribution of pore size in the real porous rocks.

SEISMOELECTRIC SIGNALS GENERATED IN POROUS ROCKS

Based on the principles of the electroseismic and seismoelectric conversions, we know these two effects are reversible. An electric current can induce a seismic wave in a porous rock sample. A seismic wave also can induce electric field in the same rock sample. To observe this reversible phenomenon, we conduct the seismoelectric measurements with the similar setup in the water tank and with the same rock samples. Figure 11 shows the setup for the seismoelectric measurements. A power hydrophone (Model LC-34, Celesco Ind., Inc.) is used for the acoustic source and it is excited with the same single sine burst pulse that was applied as the electric source in the electroseismic measurements. The other hydrophone (B & K 8103) near the rock sample records the acoustic field around the sample. Two point measurement electrodes record the voltages (V1 and V2) across the sample, which are induced by the electric current due to the seismoelectric conversion in the samples.

No electric field can be induced in a water tank if there is no porous medium. However in our experiments, even when there is no porous medium in the water tank, the measurement electrodes still record electric noise and the interaction of the high-voltage electric source with other electronic equipment in the laboratory. Figure 12 shows the resulting electric signals when the source hydrophone is excited by the single sine burst at the different center frequencies with rock sample present. These are the background noises in our seismoelectric measurement system.

We record electric signals generated with the different samples, when the source hydrophone is excited with an electric pulse with a 100 kHz center frequency. Figure 13 shows the acoustic field near the sample (trace 1), the electric field without any sample (trace 2), and the electric fields with the samples of Lucite plate (trace 3), aluminum plate (trace 4), limestone (trace 5), and Berea

sandstone (trace 6). The acoustic wave (trace 1) is recorded by the measurement hydrophone (B & K 8103). The electric signals are recorded with the measurement electrode (V1). Comparing the electric signals in traces 2-6 with the acoustic wave (trace 1), we cannot see any seismoelectric signals in the Lucite and aluminum samples (traces 3-4), but we see electric signals in trace 5-6, whose arrival times are the same as the acoustic wave in trace 1. This measurement shows the seismoelectric conversion in porous rock samples. Next we conduct more experiments to confirm that the electric signals are indeed generated by the acoustic wave in the rock sample.

When the Berea sandstone and the electrodes move in the water tank (Figure 14a), we record the electric signals with one (V1) of the point measurement electrodes (Figure 14b). The amplitude of the electric signals in Figure 14b remains constant while the apparent velocity is equal to the water velocity of 1480 m/s. Based on the arrival time and the distance between the source hydrophone and the rock sample, we confirm that the electric signals are generated by the acoustic wave propagating to the rock followed by the seismoelectric conversion in the rock sample.

We measure the seismoelectric signals in the Berea sandstone and Westerly granite in the system shown in Figure 11. Figure 15 shows the acoustic field near the Berea sandstone (Figure 15a) and Westerly granite (Figure 15b) generated by the source hydrophone at the different frequencies. Figure 16 shows the electric signals recorded with the measurement electrodes V1 (blue) and V2 (black) across the Berea sandstone (Figure 16a) and Westerly granite (Figure 16b). We record the strong electric influences of the source before 0.2 ms in Figure 16. The phases of the influences across the samples are identical, and the amplitudes are slightly different. The seismoelectric signals of V1 (blue) and V2 (black) are recorded around the arrival time of the acoustic source wave (around 0.32 ms in Figure 16a and around 0.26 ms in Figure 16b). The seismoelectric signals recorded across a sample at a certain frequency have the same amplitudes and the opposite phases. This phenomenon shows that these signals are induced inside the rock samples due to seismoelectric conversion. The porous rock is equivalent to an electric source with the same electric potential and opposite polarization across the rock, and it is generated by the acoustic field at varying frequencies. Because the porosity of the granite sample (0.8%) is much less than Berea sandstone (19.9%), the amplitude of the seismoelectric signals in the granite is weaker than in Berea sandstone.

Based on the acoustic amplitudes ($\Delta P(\omega)$) in Figure 15 and the amplitudes of the seismoelectric signals ($\Delta V(\omega)$) in Figure 16 at the different frequencies, we can calculate the normalized seismoelectric coupling coefficients ($\Delta V(\omega)/ \Delta P(\omega)$).

Figure 17 shows the seismoelectric coupling coefficients in Berea sandstone (Figure 17a) and Westerly granite (Figure 17b) in the frequencies from 15 kHz to 150 kHz, together with the theoretical results calculated with Equation 1. The experimental results with Berea sandstone in Figure 17a show the same variation as the theoretical coupling coefficient. There is some difference between the experimental and theoretical results in Figure 17b due to the small amplitudes of seismoelectric signals.

CONCLUSIONS

Because an acoustic signal is generated by the electric currents around electrodes, it is very important to separate this acoustic wave from any electroseismic signals related to porous medium measurements. We test the background noises in the measurement system, and put the different samples at a variety of distances from the source to confirm that the recorded signals are based on the electroseismic and seismoelectric conversions. The electroseismic and seismoelectric signals can be effectively separated from huge source influences and other background noises. We investigate the electroseismic and seismoelectric conversions in different rock samples with our water tank measurement system in the frequency range from 15 kHz to 150 kHz. In the electroseismic experiment, the electric field generated by a single sine pulse induces a seismic wave in water-saturated porous rock samples. In the seismoelectric experiment, the seismic wave generated by a hydrophone excited with the same single sine pulse induces an electric signal in the samples. We measure the frequency responses of the electroseismic and seismoelectric conversions and compared them with theoretically predicted coupling coefficients. The measurement results show the possible relationship between the pore sizes and the frequency-dependent coupling coefficients. The experiments and measurement system provide a method to further investigate the properties of electroseismic and seismoelectric conversions in a rock sample, such as the relationship between the conversion and fluid conductivity, temperature, PH value, etc.

ACKNOWLEDGEMENTS

REFERENCES

Deckman, H., E. Herbolzheimer, and A. Kushnick, 2005, Determination of electrokinetic coupling coefficients: 75th Annual International Meeting, SEG, Expanded Abstracts, 561-564.

Mikhailov, O. V., M. W. Haartsen, and M. N. Toksöz, 1997, Electroseismic investigation of the shallow subsurface: Field measurements and numerical modeling: Geophysics, **62** 97-105.

Mikhailov, O. V., J. Queen, and M. N. Toksöz, 2000, Using borehole electroseismic measurements to detect and characterize fractured (permeable) zone: Geophysics, **65,** 1098-1112.

Morgan, F. D., E. R. Williams, and T. R. Madden, 1989, Streaming potential properties of Westerly granite with applications: Journal of Geophysical Research, **94**, 12449-12461.

Pride, S., 1994, governing equations for the coupled electromagnetics and acoustics of porous media: Phys. Rev. B, **50**, 15678-15696.

Pride, S. R., and M. W. Haartsen, 1996, Electroseismic wave properties: J. Acoust. Soc. Am., **100**, 1301-1315.

Reppert, P. M., and F. D. Morgan, 2002, Frequency-dependent electroosmosis: J. of Colloid and Interface Science, **254**, 372-383.

Thompson, A. H., 2005, Electromagnetic-to-seismic conversion: successful developments suggest viable application in exploration and production: 75th Annual International Meeting, SEG, Expanded Abstracts, EM2.5, 554-556.

Thompson, A. H., S. Hornbostel, J. Burns, T. Murray, R. Raschke, J. Wride, P. McCammon, J. Sumner, G. Haake, M. Bixby, W. Ross, B. White, M. Zhou, and P. Peczak, 2005, Field tests of electroseismic hydrocarbon detection: 75th Annual International Meeting, SEG, Expanded Abstracts, EM2.8, 565-568.

Zhu, Z., C. H. Cheng, and M. N. Toksöz, 1994, Electrokinetic conversion in a fluid-saturated porous rock sample: 64th Annual International Meeting, SEG, Expanded Abstracts, SL1.1, 1057-1060.

Zhu, Z., M. W. Haartsen, and M. N. Toksöz, 1999, Experimental studies of electrokinetic conversions in fluid-saturated borehole models: Geophysics, **64**, 1349-1356.

Zhu, Z. and M. N. Toksöz, 2003, Crosshole seismoelectric measurements in borehole models: Geophysics, **68**, 1519-1524.

Zhu, Z. and M. N. Toksöz, 2005, Seismoelectric and seismomagnetic measurements in fractured borehole models: Geophysics, **70**, F45-F51.

(a)

100cm
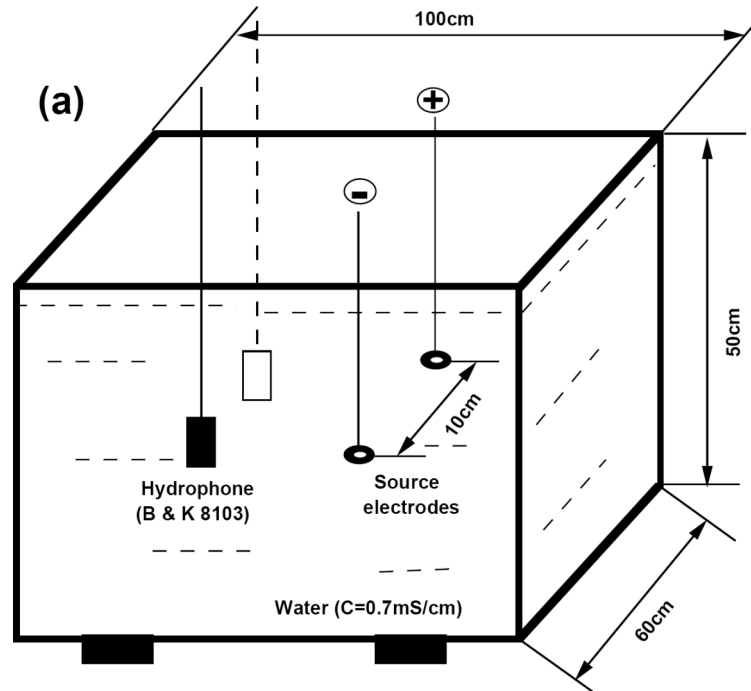
(b) Overview of water tank
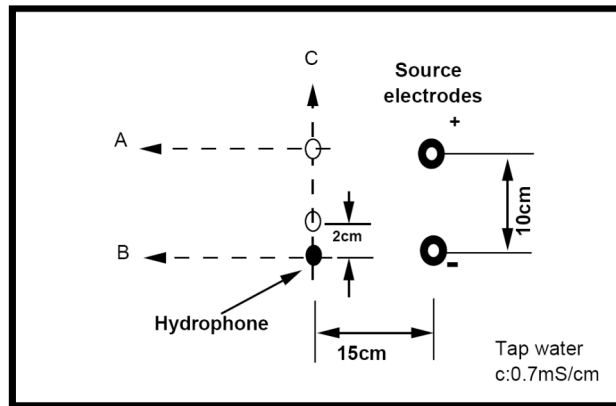
Figure 1: Schematic diagram of electroseismic measurements in a water tank (Figure 1a). The ring electrodes are made from brass wire. An electric pulse square pulse with 250 V in amplitude and 6 μs in width is applied to the electrodes separated by 10 cm. A hydrophone of Type B & K 8103 moves along the lines A, B, and C (Figure 1b) to record the acoustic waves.
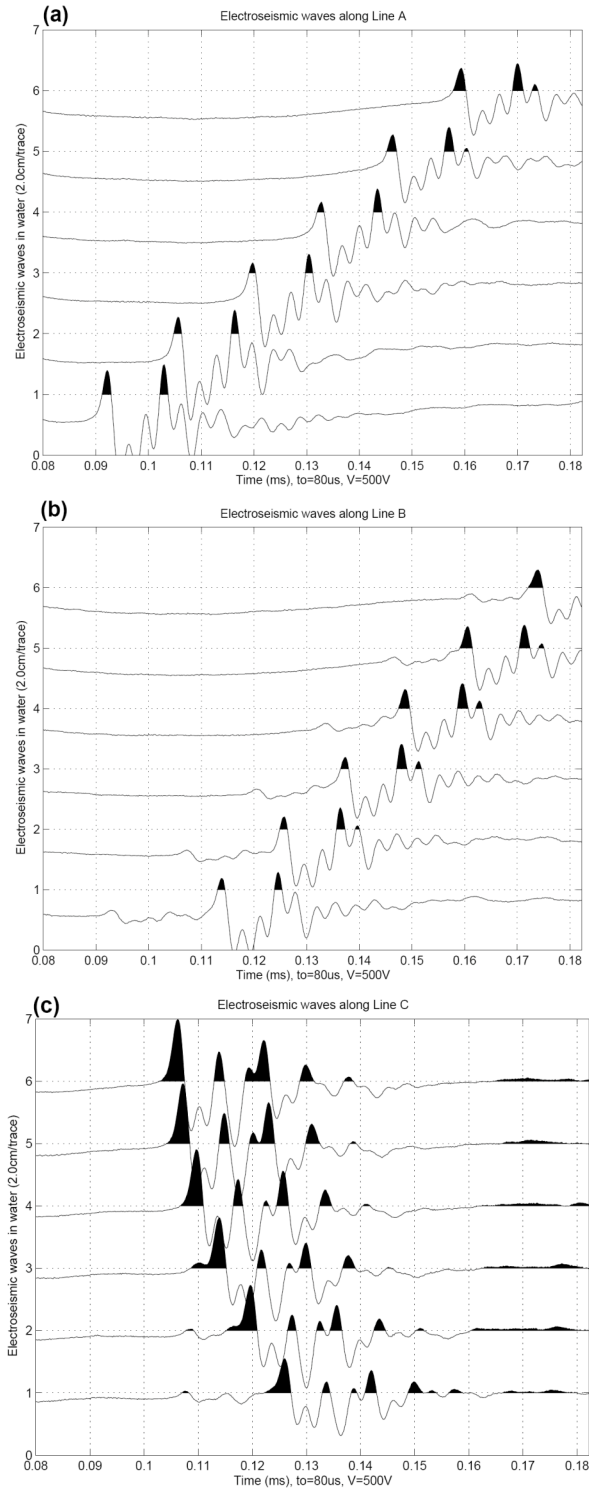
Figure 2: Seismic waveforms recorded in the water tank (Figure 1) when the hydrophone moves along Line A (a), Line B (b), and Line C (c). Two acoustic waves with differing amplitudes are induced around the positive and negative electrodes, respectively.

(a)

(b)
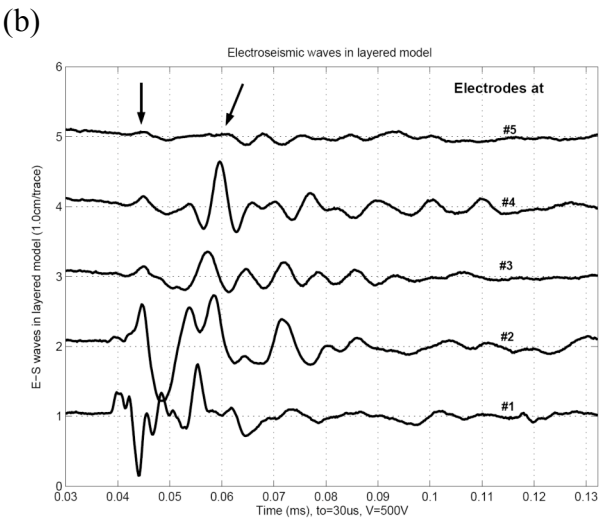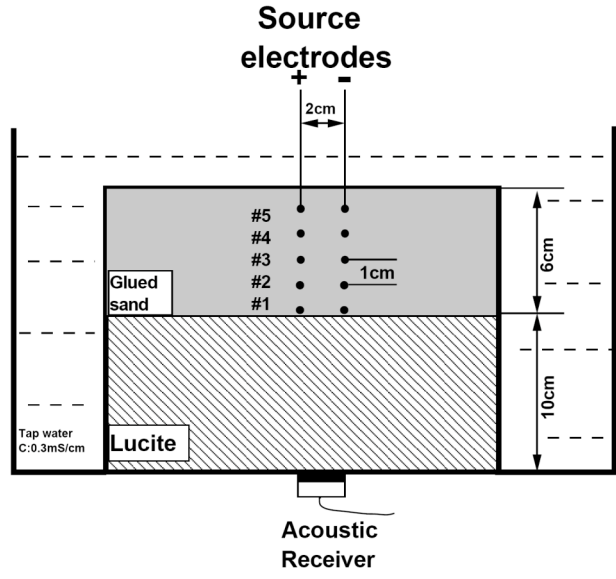
Figure 3: A layered model with epoxy-glued sand and Lucite block saturated with tap water of 0.7 mS/cm in conductivity (Figure 3a). Five pairs of the electrodes are buried in the sand. An electric square pulse with 500 V in amplitude and 6 μs in width is applied to the electrodes and an acoustic P wave transducer records the electroseismic waves on the bottom surface of the Lucite block. Electroseismic waveforms (Figure 3b) are recorded with the transducer when the electrodes at different depth are excited. Two arrows indicate two seismic waves. The first, generated at the interface, arrives at the same time (0.038 ms to 0.05 ms). The second, generated at the electrodes, arrives at different times.
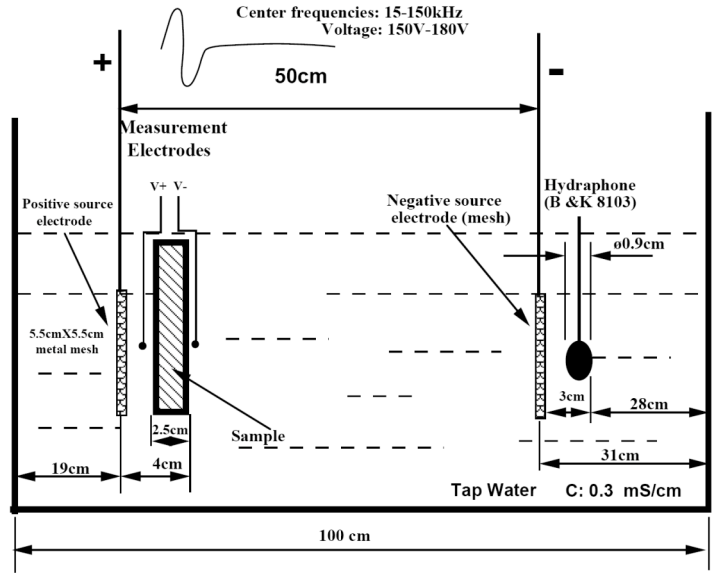
Figure 4: Schematic diagram of electroseismic measurements in a water tank. A single sine burst of 150V-180V in voltage and 15 kHz-150 kHz in frequency excites the source electrodes. The measurement electrodes record the electric potential across the sample, and a hydrophone of Type B & K 8103 measures the acoustic fields in the water tank.

13
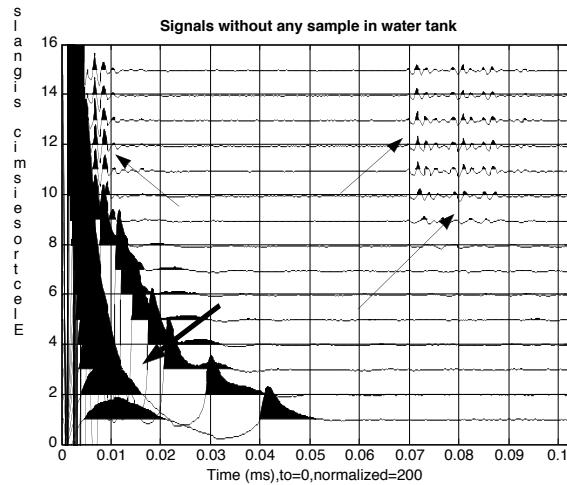
Figure 5: Acoustic field at the different frequencies recorded by the hydrophone in the water tank without any sample. The arrows indicate three points of interest: the source influence, acoustic waves generated by the positive or negative electrode, and the reflection from the water tank walls.
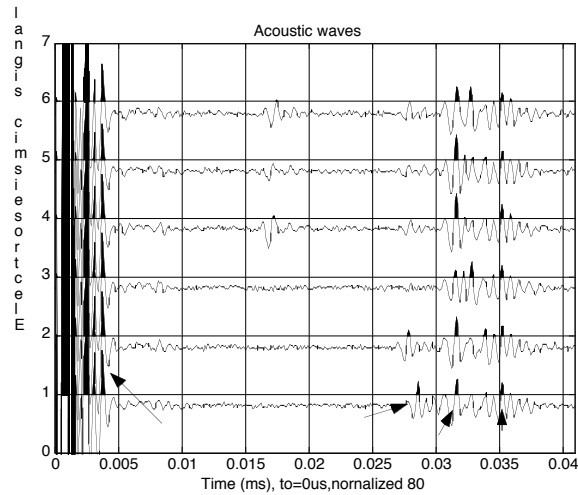
Figure 6: Acoustic waveforms when the samples are Lucite (trace 2), aluminum (trace 3), Berea sandstone (trace 4), limestone (trace 5), and Coconino sandstone (trace 6) samples (plates). The electric source is a single sine pulse with a center frequency of 100 kHz. Trace 1 is the acoustic wave without any sample.

(a)
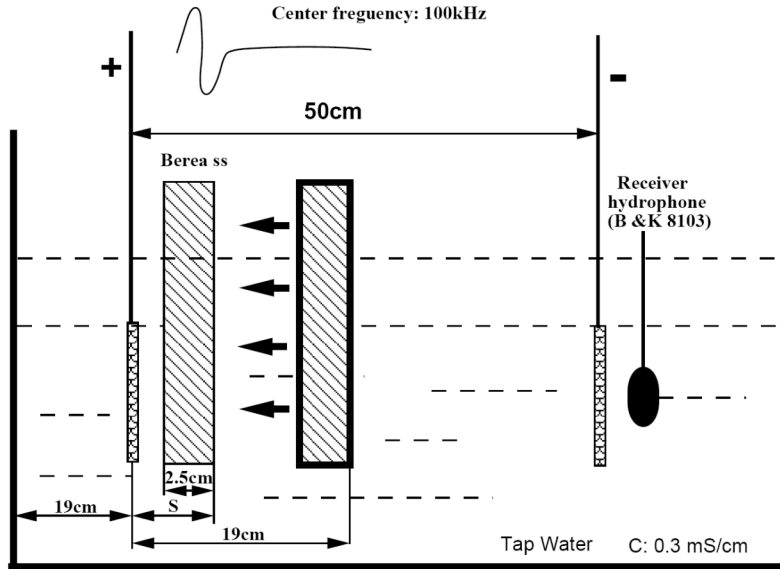
(b)
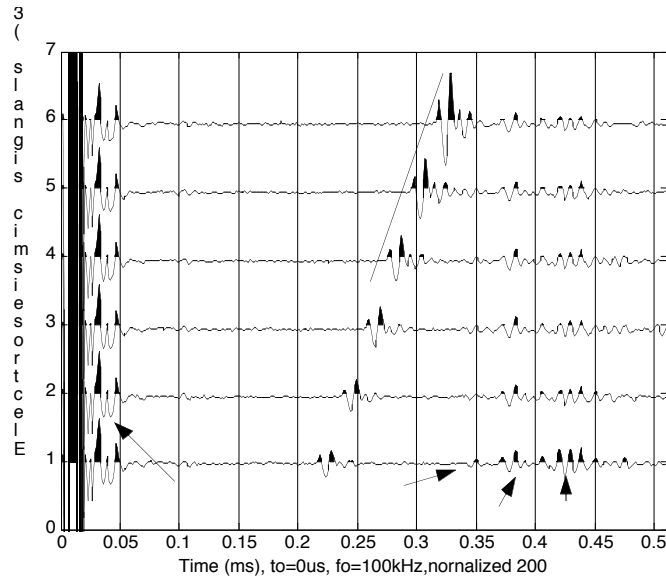
Figure 7: schematic diagram (Figure 7a) of electroseismic measurement system when a Berea sandstone sample moves between the source electrodes. The start position of the sample is 19 cm from the positive electrode and moves in increments of 3 cm. The hydrophone records the acoustic fields (Figure 7b). The arrows indicate the noise in the water tank and the sloping line shows the electroseismic signals. The apparent velocity based on the line slope is equal to the water velocity.

15

ELectroseismic waveforms in Berea sandstone

Time (ms), normalized 100
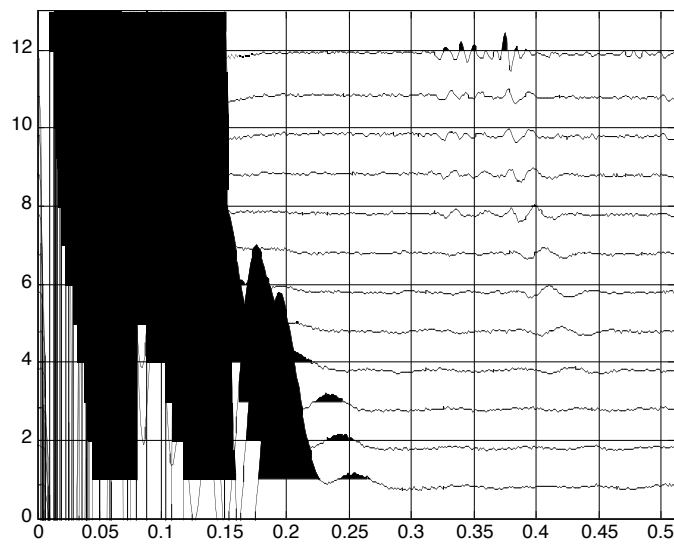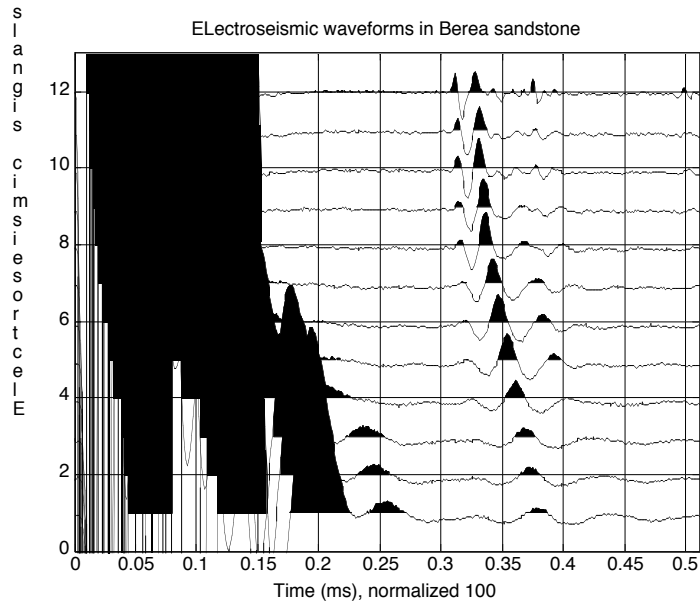
Figure 8: Electroseismic waveforms recorded with the Berea sandstone (Figure 8a) and Westerly granite (Figure 8b) samples in the water tank at frequency range from 15 kHz to 150 kHz. The waveforms with huge amplitude before 0.3 ms are the electric source influences.
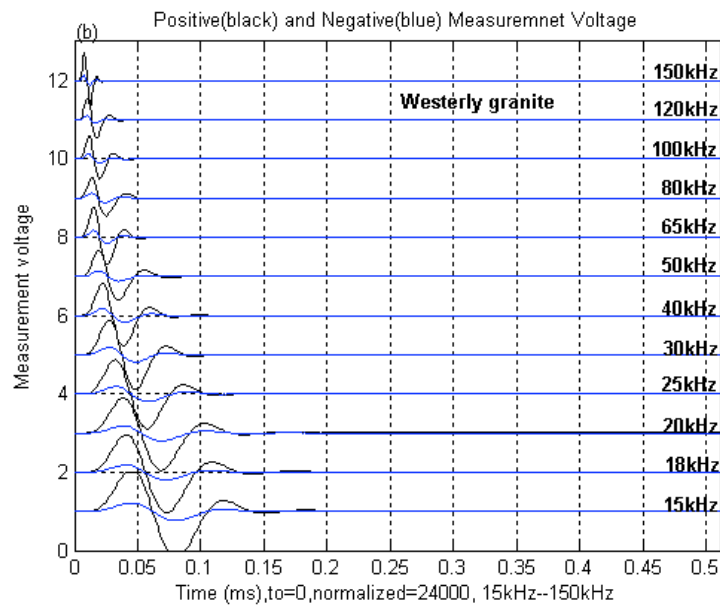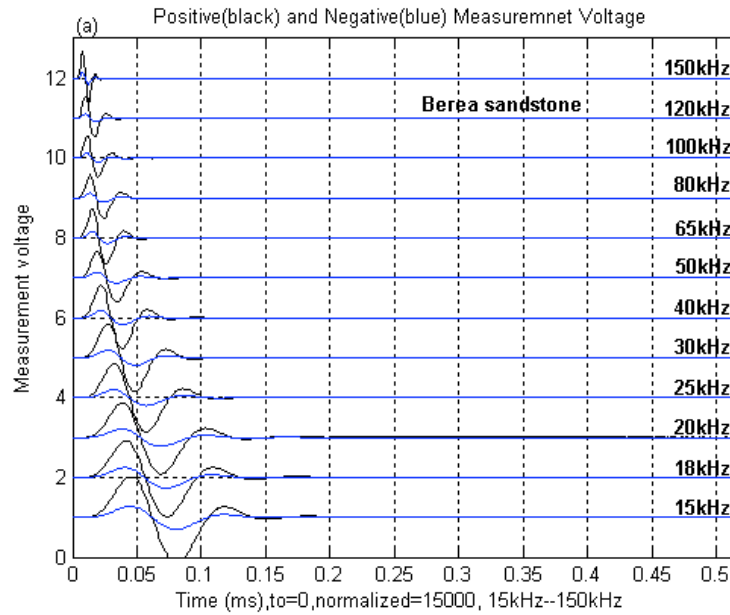
Figure 9: Electric signals recorded with measurement electrodes of V+ (black) and V- (blue) in Berea sandstone (Figure 9a) and Westerly granite (Figure 9b). The phases of the voltages V+ and V- are identical.
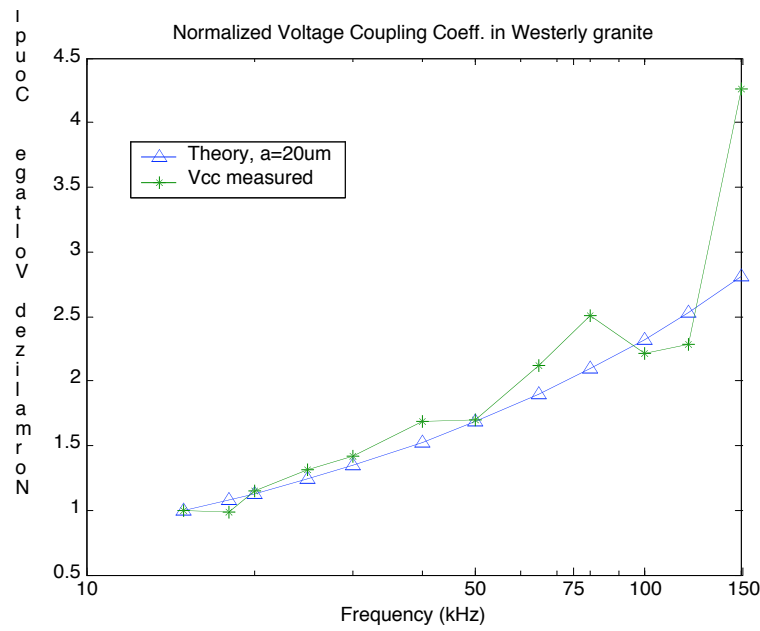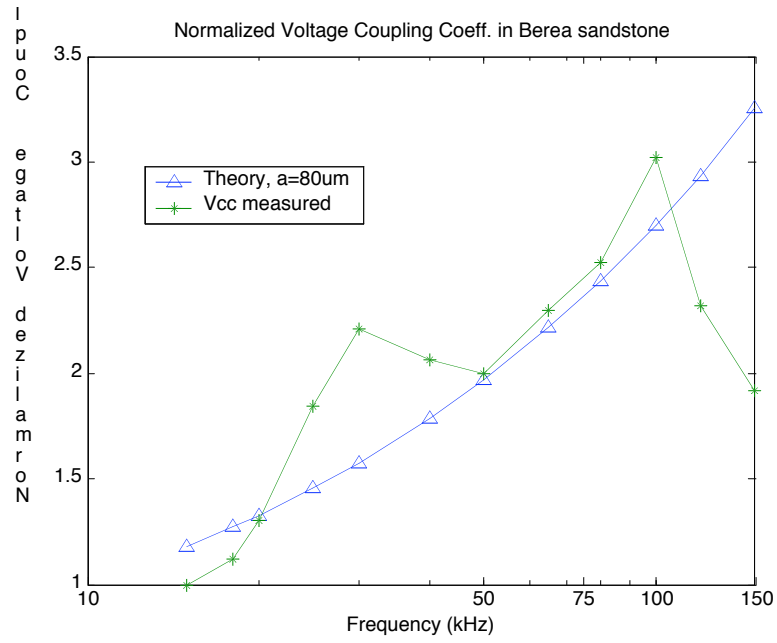
Figure 10: Normalized electroseismic voltage coupling coefficients ($\Delta P(\omega)/\Delta V(\omega)$) measured in Berea sandstone (Figure 10a) and Westerly granite (Figure 10b). The theoretical voltage coupling coefficients are calculated with the pore radius of 80 μm (Figure 10a) and 20 μm (Figure 10b).
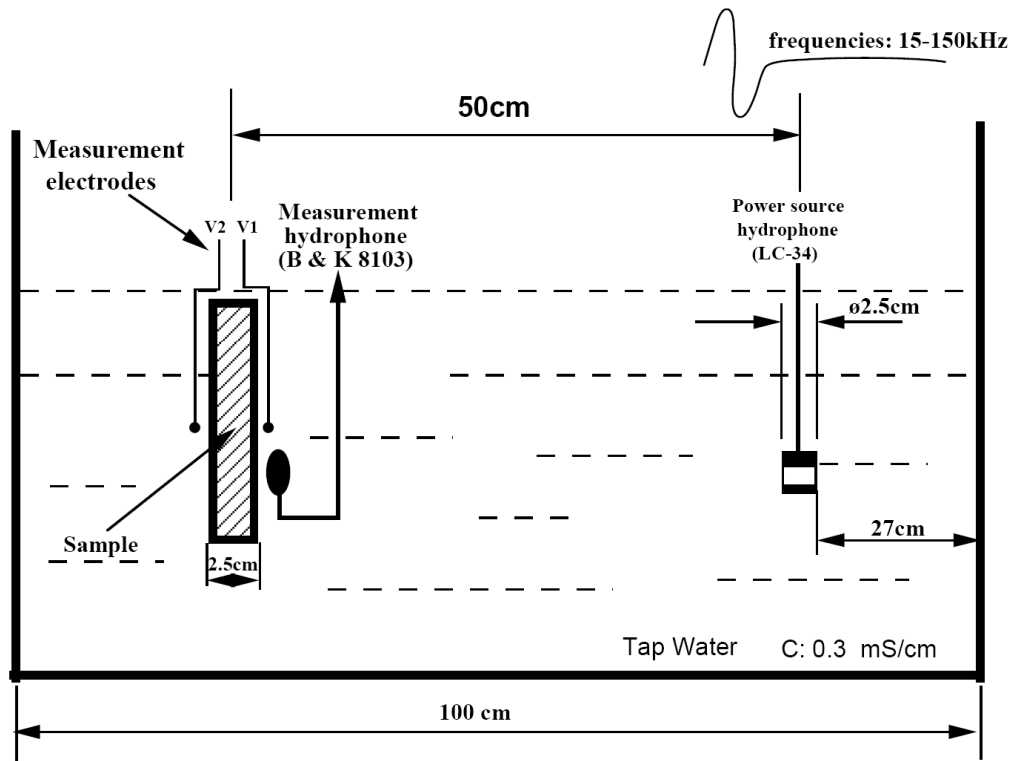
Figure 11: Schematic diagram of the seismoelectric measurements in a water tank. A single sine burst with 150V-180V in voltage and 15 kHz-150 kHz in frequency excites the source hydrophone (Model LD-34). The measurement electrodes record the electric potential across the sample. A measurement hydrophone of Type B & K 8103 is placed near the sample to measure the source acoustic wave arriving at the sample.
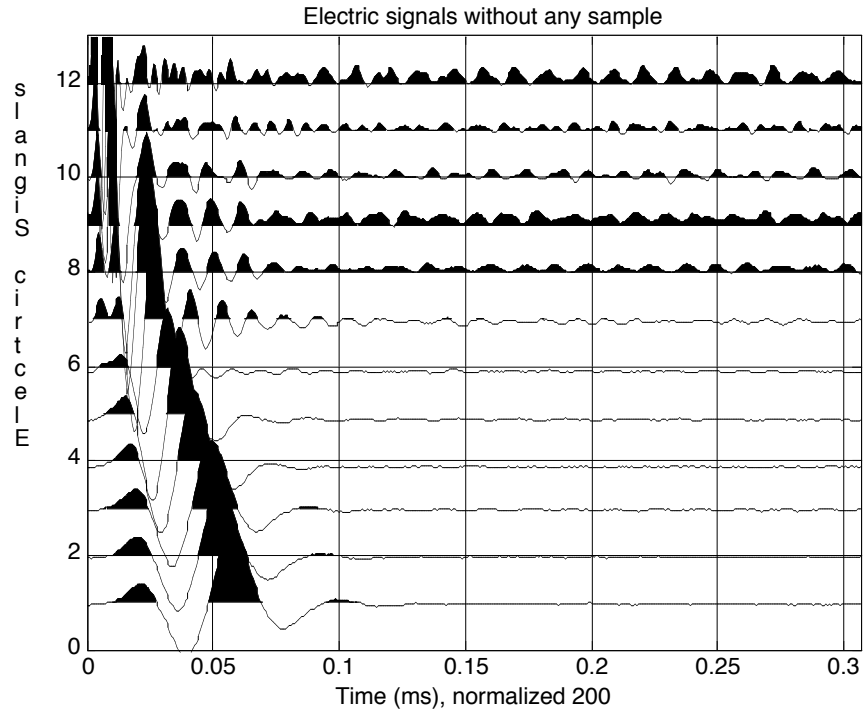
Figure 12: Background electric noise without any sample, recorded by the measurement electrode V1 in Figure 11. The frequency range is from 15 kHz to 150 kHz.
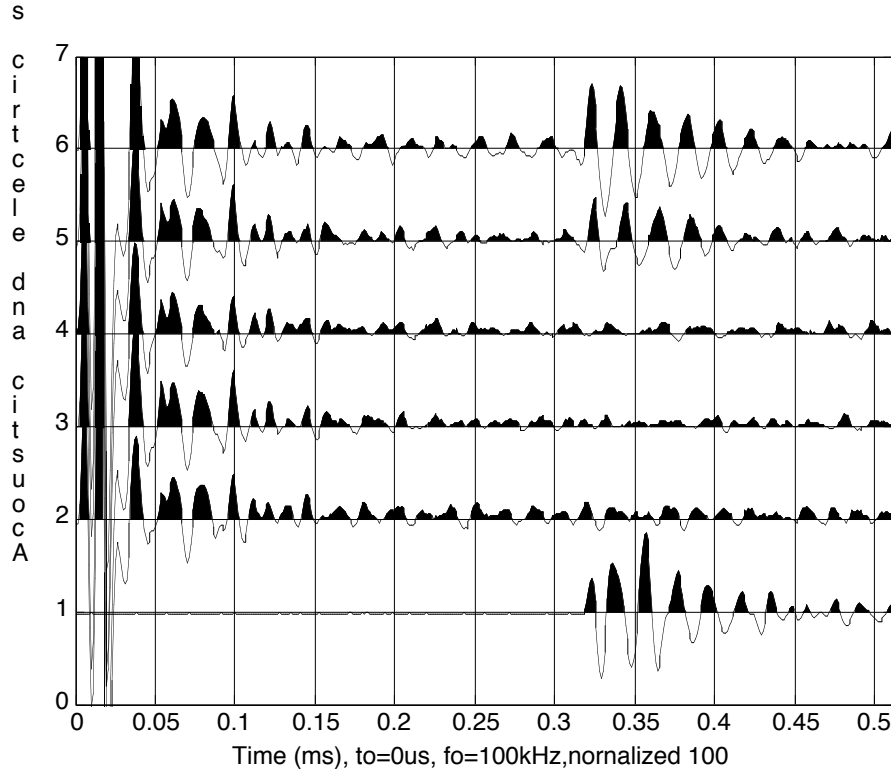
Figure 13: Acoustic waveforms (trace 1) near the sample and the electric waveforms without any sample (trace 2), or when the samples are Lucite (trace 3), aluminum (trace 4), limestone (trace 5), and Berea sandstone (trace 6).

21
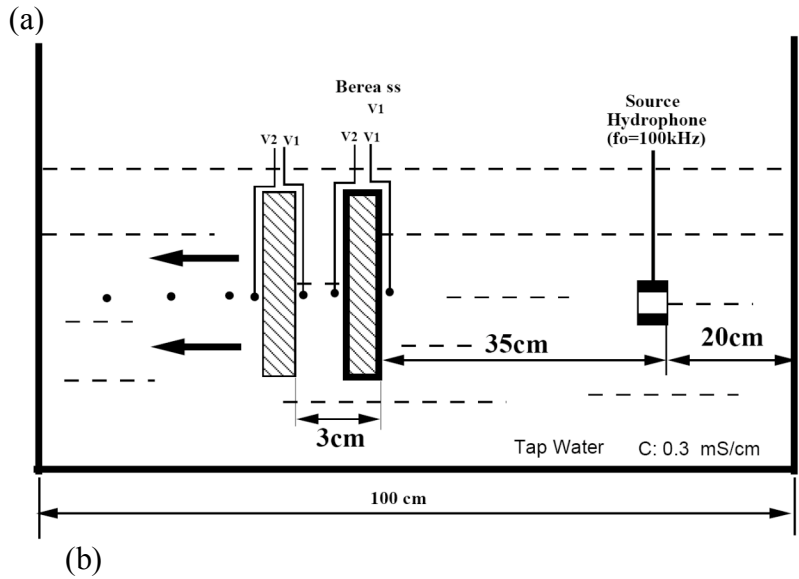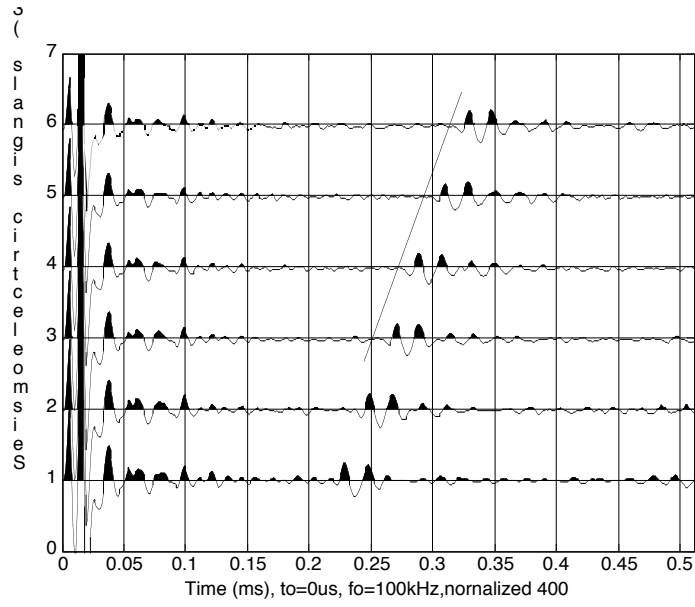
Figure 14: Schematic diagram (Figure 14a) of seismoelectric measurement system when a Berea sandstone sample with the measurement electrodes moves in the acoustic field. The measurement electrode V1 records the electric signals (Figure 14b). The sloping line indicates the seismoelectric signals, whose apparent velocity based on the line slope is equal to the water velocity of 1480 m/s.
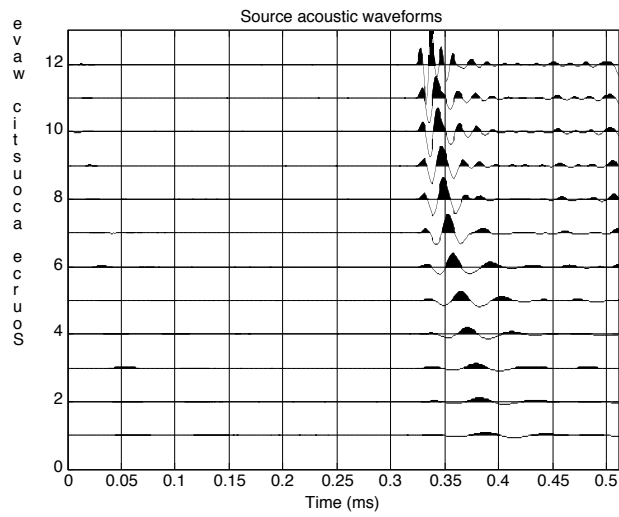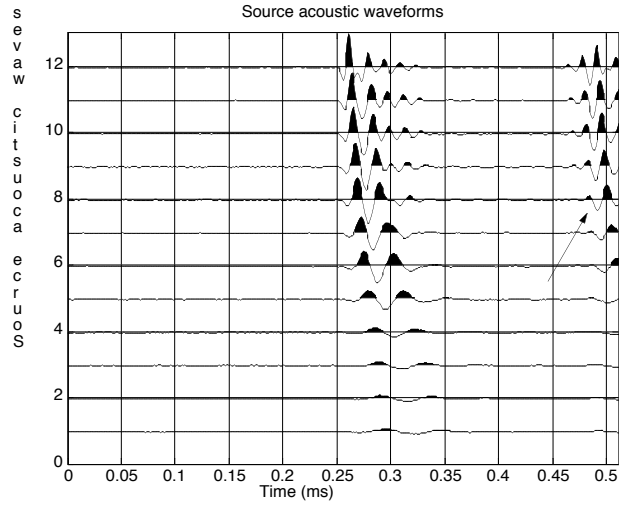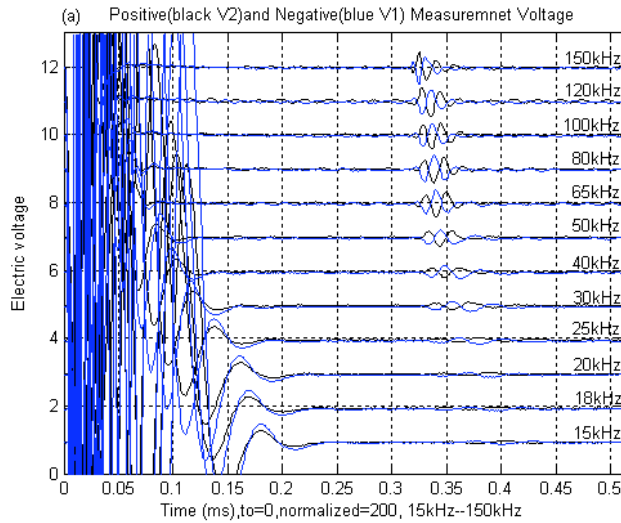
Figure 15: Acoustic waveforms near the rock samples of Berea sandstone (Figure 15a) and Westerly granite (Figure 15b) generated by the source hydrophone at the frequency range from 15 kHz to 150 kHz.
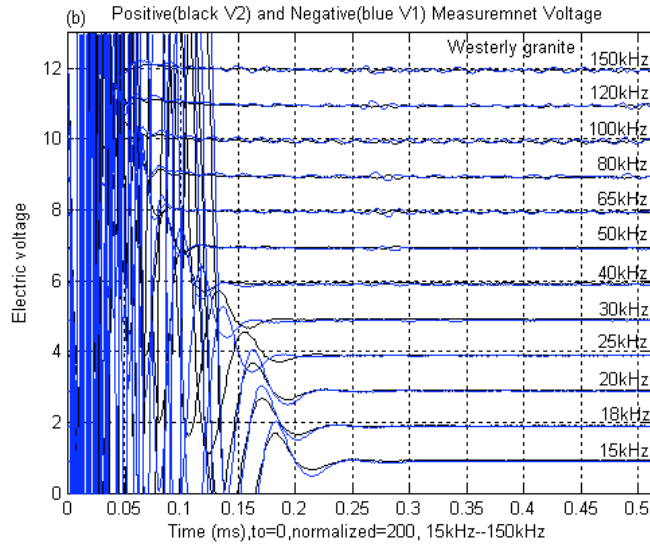
Figure 16: Electric signals recorded with the measurement electrodes V1 (blue) and V2 (black) across the Berea sandstone (Figure 16a) and Westerly granite (Figure 16b) at the frequencies from 15 kHz to 150 kHz. The source electric influences before 0.2 ms have the same phases, but the seismoelectric signals of V1 (blue) and V2 (black) have opposite phases (around 0.32 ms in Figure 16a).
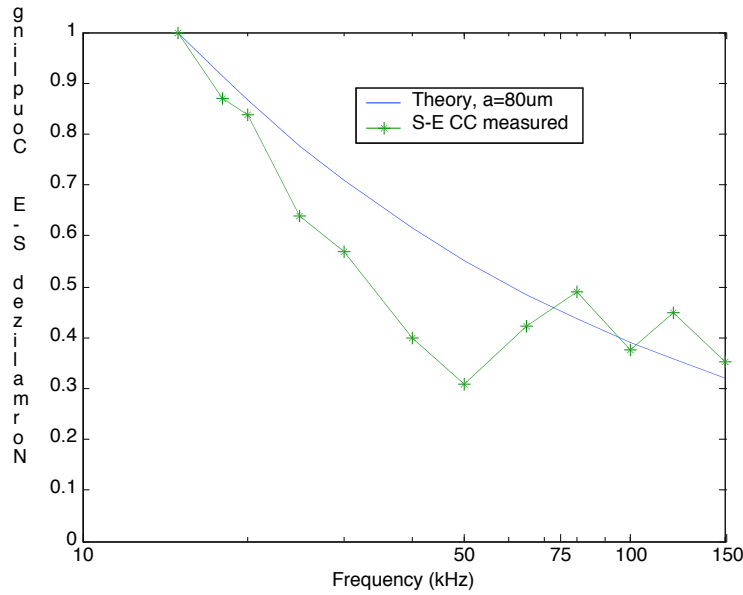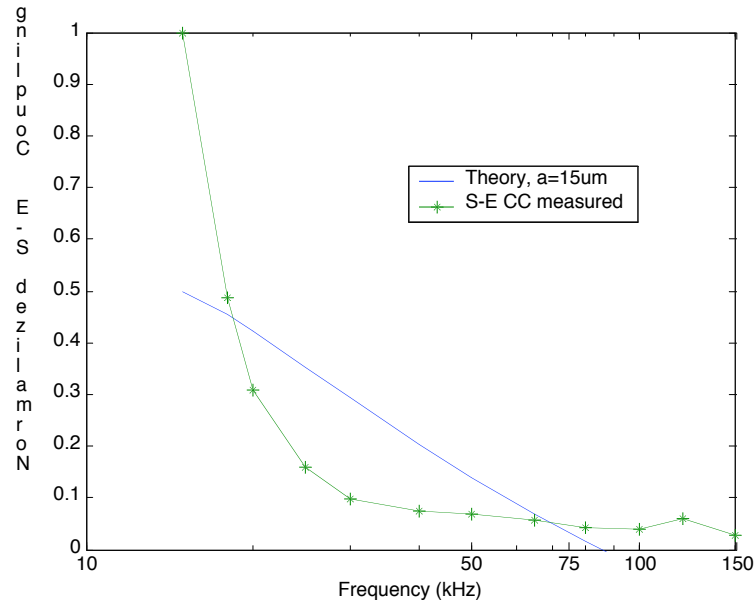
Figure 17: Seismoelectric coupling coefficients ($\Delta V(\omega)/ \Delta P(\omega)$) in Berea sandstone (Figure 17a) and Westerly granite (Figure 17b) at the frequencies from 15 kHz to 150 kHz, and the theoretical coupling coefficients calculated with the pore radius of 80 μm (Figure 17a) and 15 μm (Figure 17b).